ISBN: 978-3-95450-211-0 doi:10.18429/JACoW-SRF2019-TUP043

AB-INITIO STUDY OF ATOMIC SCALE INTERACTION AMONG Nb, Sn, Cl, AND O*

Aron Tesfamichael, Clark Atlanta University (Chemistry Department), Atlanta, USA
Tomas Arias, Cornell University (Physics Department), Ithaca, USA

Abstract

Niobium (III) Tin (Nb_3Sn) is the most promising alternative material for SRF accelerator cavities. The material can achieve higher quality factors, higher temperature operation and potentially higher accelerating gradients compared to conventional niobium. Cornell University has a leading program to produce 2 - 3 micrometer thick coatings of Nb_3Sn on Nb for SRF applications using vapor diffusion. This program has been the first to produce quality factors higher than achievable with conventional Nb at usable accelerating gradients. Here we employed a combination of ab-initio calculations and statistical mechanical models to understand the nature of atomic scale interaction among Nb, Sn, Cl, and O. Because of the profound Nature of the interaction, we began our study by focusing only on the interaction of Nb with Sn in the absence of Cl and O. Our results indicated: diffusion rate is five times slower comparing to the rate of re-evaporation, and also the time given for nucleation stage (5hr) is too short comparing to diffusion rate (200 days), this result can be supported by both charge density and electric field decrease as Sn atom is transformed from Nb surface across z-axis. Therefore, we conclude that the presence of oxides is important and also Cl impurity can't be avoided.

INTRODUCTION

Superconductivity in Nb_3Sn was discovered by Matthias et al. in 1954 [1], one year after the discovery of V_3Si, the first superconductor with the A15 structure by Hardy and Hulm in 1953 [2]. Its highest reported critical temperature is 18.3 K by Hanak et al. in 1964 [3]. Ever since its discovery, the material has received substantial attention due to its possibility to carry very large current densities far beyond the limits of the commonly used NbTi. It has regained interest over the past decade due to the general recognition that NbTi, the communities' present workhorse for large scale applications, is operating close to its intrinsic limits and thus exhausted for future application upgrades. Nb_3Sn approximately doubles the available field-temperature regime with respect to NbTi and is the only superconducting alternative that can be considered sufficiently developed for large scale applications.

Mechanically, Nb_3Sn is brittle, and a poor thermal conductor. Deformation of a niobium surface that had been coated with Nb_3Sn resulted in extensive fracturing of the coated layer [4] and measurements of the thermal conductivity of Nb_3Sn [5] at 4.2 K is approximately 10^3 times lower than that of niobium. From an engineering standpoint, these properties result in the optimal solution for SRF cavities being a thin film coating of Nb_3Sn on some other, more thermally conductive substrate, such as niobium or copper. Nb_3Sn is an intermetallic alloy in the A15 phase, with a stoichiometric ratio of three niobium atoms to every tin. The stoichiometric crystal structure is shown in Fig. 1, with the elements marked.

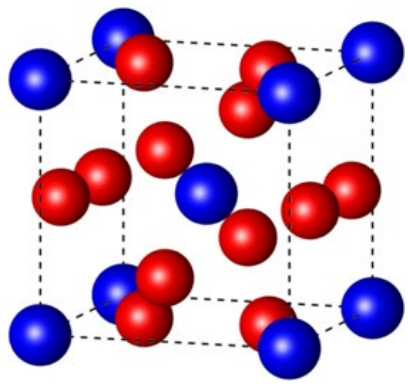

Figure 1: The unit cell of A15 Nb_3Sn, showing the tin atoms in blue and the niobium atoms in red.

Nb_3Sn has been well known to the superconducting magnet community for some time, and much work has already been undertaken to understand its fundamental properties. A more general review on the material properties of Nb_3Sn was published by Godeke [6]. In this section we will briefly review properties of Nb_3Sn that are most relevant to its use as a superconductor in SRF cavities.

Of primary interest when fabricating Nb_3Sn is the stoichiometry of the material produced. It has been seen, in phase diagrams published by Charlesworth [7] and more recently Feschotte and Okamoto [8,9] , that in the binary system of niobium and tin, the phase Nb_3Sn exists in pure form (without cohabitation with niobium, liquid tin, or other phases of Nb–Sn) for atomic percentages of tin between 17 and 26 percent at temperatures between 950 °C and 2000 °C. This region of solitary existence of the A15 phase is highlighted in the phase diagram shown in Fig. 2. It is this region of the phase diagram that is of interest for the fabrication of an SRF surface. Extreme tin deficiency will result in areas of uncovered niobium; excess tin will result in unreacted tin at high temperatures, or other phases of Nb–Sn at lower temperatures. These low-T_c tin-rich phases are expected to have a far higher RF surface resistance than niobium.

Nb_3Sn has been well known to the superconducting magnet community for some time, and much work has already been undertaken to understand its fundamental properties. A more general review on the material

ISBN: 978-3-95450-211-0 doi:10.18429/JACoW-SRF2019-TUP043

properties of Nb_3Sn was published by Godeke [10]. In this section we will briefly review properties of Nb_3Sn that are most relevant to its use as a superconductor in SRF cavities.

It is not sufficient, however, that the material produced lie in the range of 17–26 atomic percent tin, as the superconducting properties of Nb_3Sn are a function of the atomic percent tin content. Crucially, the transition temperature T_c decreases significantly for atomic percentages of less than 23 percent tin. A plot showing the dependence of this transition temperature on the atomic percent tin, originally published in [10], is shown in Fig. 3. From this, it can be surmised that, for best performance, the region of the phase diagram that must be achieved lies between 23 and 26 atomic percent tin.

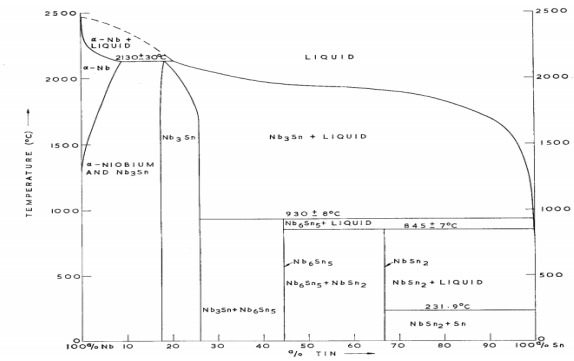

Figure 2: The phase diagram of the niobium–tin system, as measured by Charlesworth in 1970 (adapted from [10]).

FABRICATION OF Nb_3Sn USING VAPOR DIFFUSION

The coating furnace designed at Cornell University, at least in part, is a replication of the furnace design of both Siemens and Wuppertal Universities. However, the Cornell design incorporates a second heating element around the tin source, allowing the tin source to be held at a higher temperature than the part to be coated. Simplified diagrams of the furnaces used at Cornell is shown in Fig. 4. Demonstrates all the steps utilized to date:

A degas stage The chamber is taken to a temperature between 100-200 °C and parked at this temperature. During this time, active pumping on the chamber removes residual moisture, etc., that may have been introduced during the opening of the furnace and the placing of the part.

A nucleation stage At this stage, the chamber is taken to an intermediate temperature, during which time nucleation sites are created on the surface of the substrate. Historically, this has been done either by pre-anodization and the introduction of a temperature gradient during the ramp-up (Siemens) [11], or the use of a nucleation agent such as SnF_2 (Siemens) or $SnCl_2$ (Siemens, Wuppertal, Cornell, Jefferson Lab) [12]. Using a nucleation agent instead of pre-anodization helps to prevent uncovered areas, but avoids the RRR degradation that has been observed after growing a thick oxide and then diffusing it into the bulk of the niobium substrate [13].

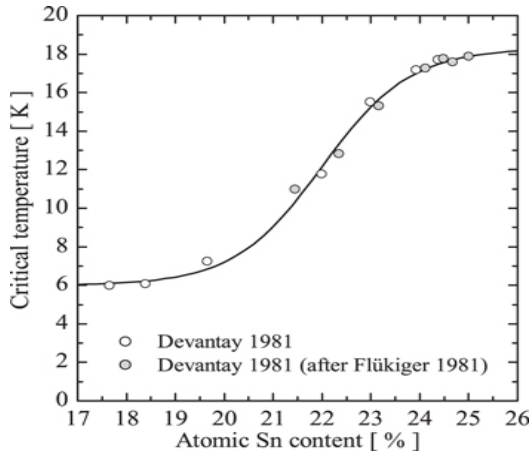

Figure 3: A plot of the critical temperature of Nb_3Sn as a function of the atomic percent tin content, fitted to a Boltzmann function. This plot has been adapted from [10].

Ramp to coating temperature Beginning from the intermediate temperature of the nucleation stage, the secondary heating element is often activated at this stage, if it is present. The chamber is then increased to the desired coating temperature.

The coating stage The cavity is held at a constant temperature above 950 °C, at which temperature the low-Tc phases of Nb-Sn (Nb_6Sn_5 and $NbSn_2$) are thermodynamically unfavorable. During this phase, the layer grows on the surface of the niobium, as tin consumed in the production of the layer is replenished by the tin source. During this stage, the tin source is held at a temperature higher than the part, in the event that a secondary heating element around the tin source is present.

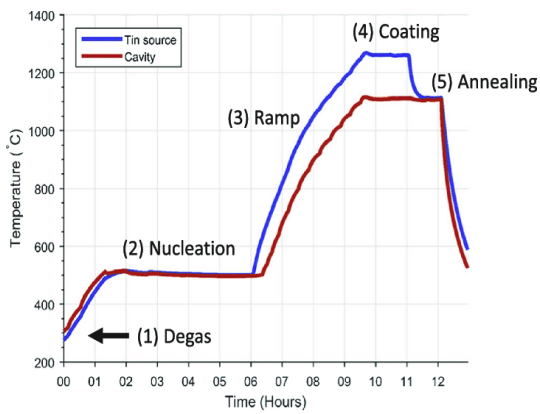

Figure 4: Temperature of profiles of coating furnace used by Cornell.

An annealing stage In the event that a secondary heater is not present, this stage is likely to be identical to the coating stage. If a secondary heater is present, then it is closed and/or turned off and allowed to cool, thus reducing the rate of tin arriving at the surface of the part. During this

ISBN: 978-3-95450-211-0 doi:10.18429/JACoW-SRF2019-TUP043

time, the chamber is held at a temperature above 950 °C, often at the same temperature at which it was held during the coating stage. The purpose of this step is to allow any excess of pure tin at the surface of the part to diffuse into the layer and form Nb_3Sn.

Virtually all temperature profiles published to date can be described using a succession of these five stages, although the first two steps – degas and nucleation – are sometimes omitted. Furthermore, in the absence of a secondary heater, the coating and annealing stage are often indistinguishable from one another based on the temperature profile alone.

Here we present an update on progress at Cornell University theoretical studies of the formation of the Nb_3Sn layer using density functional theory calculations for binding energy, diffusion rate, activation energy, re-evaporation rate, electric field as well as oxidation state change as Sn atom is transported from Nb layer.

COMPUTATIONAL METHODS

All bulk crystal, vacancy and interstitial properties have been calculated using the Vienna ab-initio Simulation Package (VASP). In these calculations, we used the projector augmented wave (PAW) method with a plane wave cut-off 350 eV for vacancy and interstitial calculations. The calculations were spin-polarized and the Perdew–Burke–Ernzerhof parameterization of the generalized gradient approximation (GGA) was used for the exchange–correlation potential. The PAW potentials were generated using the following electronic configurations: $4d^4\ 5s^1$ for Nb and $4d^{10}\ 5s^2\ 5p^2$ for Sn. The cell shape and volume are kept fixed to that of pure Nb with a bcc structure but internal ionic relaxations are allowed. Brillouin-zone sampling was conducted using the Monkhorst and Pack scheme. A 4x4x4 k-points mash at a temperature of 1050 ºC was employed for calculation.

OBJECTIVE

The objective of this study have been focused on understanding the cause of Nb_3Sn coatings on Nb imperfection, which are anticipated to have significant detrimental effects on the performance of Nb_3Sn coated cavities: patchy regions with extremely thin grains [5-7] and Sn-deficient regions.

Nb_3Sn-coated cavities have been seen to quench superconductivity in the 14–17 MV m^{-1} range and some cavities still display a Q-slope, the increase of surface resistance as a function of accelerating field. The surface magnetic field at which the quench occurs, ~70 mT is, however, significantly lower than the superheating field of Nb_3Sn at ~400 mT, the ultimate limit predicted by the theory for an RF superconductor with an ideal surface [9-11]. These limits have been suggested to be a consequence of imperfections in the Nb_3Sn coatings [12], including surface roughness, thin regions, Sn-deficient regions, grain boundaries, and surface chemistry. For the purpose of study we have employed ab-initio calculations: (I) to compare surface diffusion barrier vs absorption barrier and annealing rate with both diffusion and absorption rate (II) effect of impurity such as the presence of chlorine in the substrate and oxidation of bulk niobium, (III) electric field potential and (IV) change of charge density as Sn is transports across Nb surface.

RESULTS AND DISCUSSIONS

Diffusion Barrier vs. Re-Evaporation Barrier

Coating of Nb_3Sn on Nb for SRF applications using vapor diffusion is depending on many factors such as thickness, composition and morphological evolution of the product phase. Morphological evolution in the diffusional zone depends on many factors. Among them are the annealing temperature and time, relative mobilities of the species, number of nucleation sites and so on. Further increase in the grain size along with the growth of the product layer makes the whole process very complicated. In this study we have calculated the re-evaporation barrier using equation 1:

$$\nu = \nu_0 \exp(-E_b/K_bT) \quad (1)$$

where: ν_0 - Initial time of contact between the reactants or Attempt frequency $10^{13}s^{-1}$, E_b - activation energy (evaporation barrier) in eV unit, K_b - Boltzmann constant, $8.61733034 \times 10^{-5}$ eV/K; T- Temperature, 1123 K.

To calculate the activation energy (E_b) one Sn atom was transported from bulk Nb layer in z-axis by keeping the x-y plane constant as in Fig. 5a. The graph shows binding energy (eV) Vs. Sn transport (Aº). The activation energy was obtained by subtracting the binding energy between Nb layer and Sn atom at the immediate contact from the binding energy at which Sn atom is completely isolated from the Nb layer in this case the result is ~4.7 eV. Once the activation energy was obtained the evaporation barrier was calculating using equation 1. For this specific interaction the rate of re-evaporation was calculated to be ν ~0.001042 S^{-1} this implies t ~960 hrs or ~40 days. Also Fig. 5b illustrated the electron density spectra of both Nb and Sn as they are decomposed.

Similarly, we calculated the change in electron density or oxidation state change of Sn as it is transported from bulk Nb in the z-axis as shown in Fig. 5c. Our result indicates the electron density is reduced exponentially as it is moving apart from Nb layer which implies there is a covalent bonding between Sn and Nb in addition to intermetallic interaction and it can be concluded that Sn is oxidized and Nb is reduced as they interact. On the other we also calculated the electric field change as Sn is transported from bulk Nb using Maxwell equation 2.

$$E = K(q)^2/z \quad (2)$$

where: E is electric filed, K coulomb constant, and z-separation between the charge density Aº.

ISBN: 978-3-95450-211-0 doi:10.18429/JACoW-SRF2019-TUP043

Our result as shown in Fig. 5d illustrated clearly that there is a linear decrease of electric field of Sn as it is transported from the surface of Nb layer and it is a perfect agreement with Maxwell Equation.

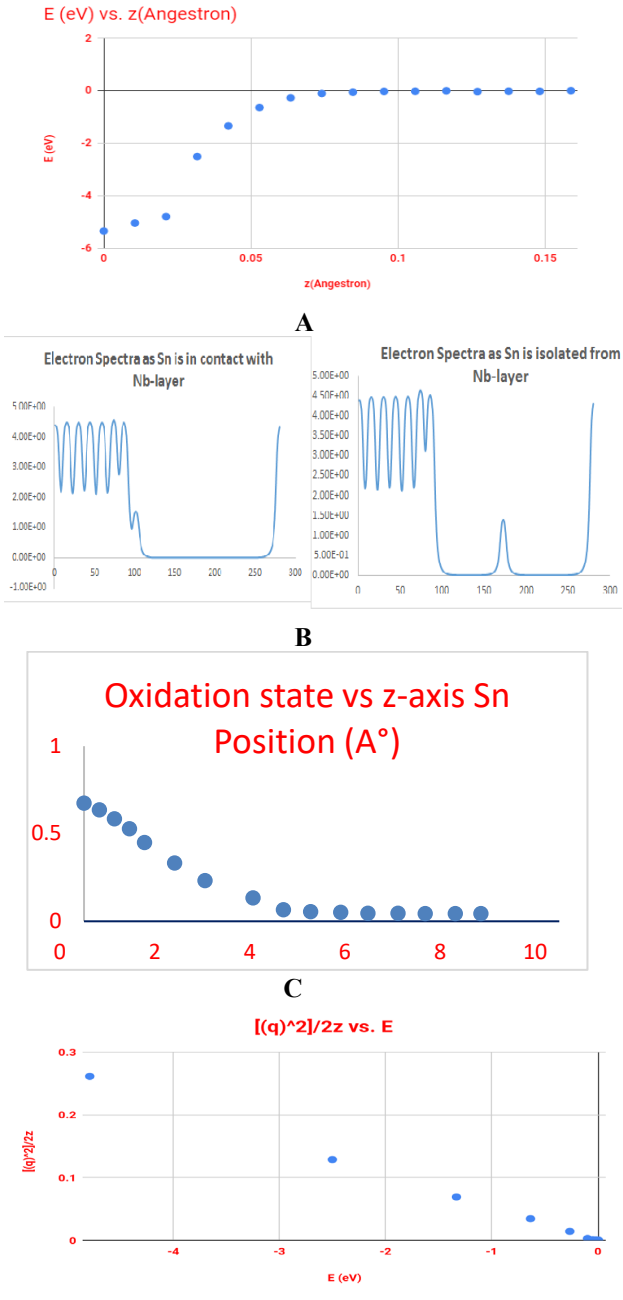

Figure 5: (a, b, c, and d) binding energy, electron density spectra, electron density change of Sn, respectively as it is transported across z-axis from Nb layer.

Our next step was to calculate the Diffusion barrier using equation 3 and 4 and compare with Re-evaporation barrier and time of annealing at constant temperature:

$$D = a^2 \nu \exp(-Ea/K_bT) \quad (3)$$

where: D - diffusion rate, a - lattice length 3.14 (10^{-10}) m, ν - Initial time of contact between the reactants or attempt frequency $10^{13} s^{-1}$, Ea - activation energy (diffusion barrier), T- temperature, and K_b- Boltzmann constant.

For the purpose of calculation one Sn atom was transported along x-y plane by keeping the z-axis constant and binding energy vs. separation distance was plotted as shown in Fig. 6. Then activation energy was calculated by subtracting the binding energy at the saddle point from the minimum point of the periodic function which is approximately 1.6 eV. Diffusion barrier (D~7.72 (10^{-13})m^2 s^{-1}) was obtained by inserting the variables on equation 3.

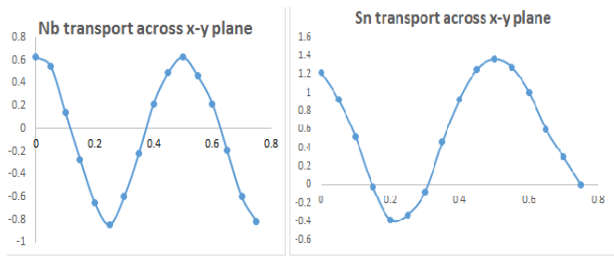

Figure 6: (a) and (b): Electron density of Sn and Nb atoms as transported across x-y axis, respectively.

Finally, diffusion rate was calculated using equation 4:

$$t = [L^2/D] \quad (4)$$

where: L (0. 5m) is the length of the cavity. So the time needed to diffuse Sn across the cavity requires ~ 4860 hr or 200 days. Therefore, we can conclude that the rate of diffusion is 1/5 slower comparing to rate of re-evaporation. Also in the same argument both diffusion rate and re-evaporation rate are too slow comparing to the time of annealing used in the fabrication process of Nb_3Sn. This plays an important factor that can play in the imperfection of Nb_3Sn production.

Another factor we have considered for the imperfection of Nb_3Sn production.is the presence of chloride in the reactant side and we can't avoid the presence of oxides because Nb is easy to be oxidized. To illustrate the effect of both of impurity we calculate the binding energy of both chlorine and oxygen atom with Nb layer in the absence of Sn as they transport in the z-axis as shown in Fig. 7a and 7b, respectively.

The binding energy of Cl with Nb layer is approximately the same as Sn and also the binding energy of O is double comparing to Sn. Therefore, for the process of production will be complicated in the presences of these impurity. In our study we have never included any other factors as such temperature change.

ISBN: 978-3-95450-211-0 doi:10.18429/JACoW-SRF2019-TUP043

CONCLUSION

In this study we employed theoretical study to understand what other conditions can be changed to enhance the performance of the cavity. So we have studied interaction of pure Nb crystal with Sn, Cl and O using ab-initio calculation and our results show that:

1. Diffusion rate is five times slower comparing to the rate of re-evaporation. Therefore, we concluded that the rate of re-evaporation of tin from the cavity is faster than the growth rate of the Nb_3Sn in the chamber.
2. The time given for nucleation stage (5hr) is too short comparing to diffusion rate (200 days).
3. Both charge density and electric field decrease as Sn atom is transformed from Nb surface across z-axis and this is in perfect agreement with the Maxwell's electric field equation.

In conclusion, this study can be used as a bench mark to explore our understanding for the imperfection of Nb_3Sn production on Nb layer by vapor diffusion. In the future work it is very important to consider: (a). the presence of oxides because Nb is easy oxidized and there are many kinds of Nb-oxides structure, (b). the presence of Cl can't be avoided because the source of the substrate is $SnCl_2$ and the binding energy of both are comparable with Nb layer.

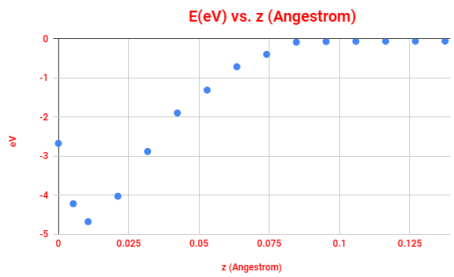

(a)

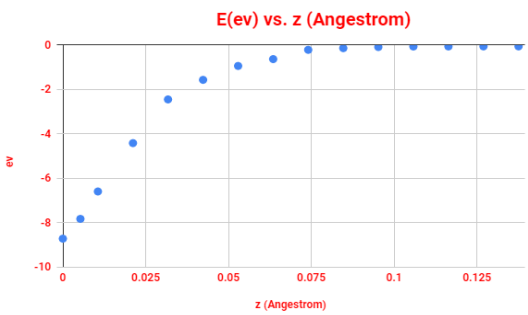

(b)

Figure 7: Oxidation state of Cl and O as it is transported across z-axis isolated from Nb-layer, respectively.

ACKNOWLEGMENT

We would like to give great appreciation to CBB for continuous support of funds.

REFERENCES

[1] B. Matthias, T. Geballe, S. Geller, and E. Corenzwit, *Phys. Rev.,* vol. 95, pp. 1435, 1954.

[2] G. Hardy and J. Hulm, *Phys. Rev*., vol. 89, pp. 884, 1953.

[3] Hanak, K. Strater, and R. Cullen, *RCA Rev*., vol. 25, pp. 342, 1964.

[4] B. Hillenbrand, "The preparation of superconducting Nb_3Sn surfaces for RF applications", in *Proc. 1st Workshop on RF Superconductivity,* Cornell Laboratory for Accelerator-Based Sciences and Education, Ithaca, USA, 1980.

[5] Y. Wang, "Fundamental Elements of Applied Superconductivity in Electrical Engineering", Beijing, China, 2013.

[6] A. Godeke, "A review of the properties of Nb3Sn and their variation with A15 composition, morphology and strain state Supercond", *Sci. Technol.*, vol. 19, R68–80, 2006.

[7] J.P. Charlesworth, I. Macphail, P.E. Madsen, "Experimental work on the niobium–tin constitution diagram and related studies", *J. Mater. Sci.* vol. 5, pp. 580–603, 1970.

[8] P. Feschotte, A. Polikar and G. Burri, "Equilibres de phases dans les systemes binaries Nb–Ge et Nb–Sn", *C. R. Seances Acad. Sci.,* C288 125–8, 1979.

[9] H. Okamoto, "Nb–Sn (niobium–tin) Binary Alloy Phase Diagrams", *Materials Park, OH: ASM International,* 1990.

[10] A. Godeke, "A review of the properties of Nb_3Sn and their variation with A15 composition, morphology and strain state Supercond", *Sci. Technol.*, vol. 19 R68–80, 2006.

[11] B Hillenbrand, "The Preparation of Superconducting Nb_3Sn Surfaces for RF applications", In *Proceedings of the First Workshop on RF Superconductivity,* Karlsruhe, Germany, pp. 41-52, 1980.

[12] B Hillenbrand, Y Uzel, and K Schnitzke. "On the preparation of Nb3Sn-layers on monocrystalline Nb-substrates", *Applied Physics,* vol. 23(3), pp. 237–240, 1980.

[13] D. Dasbach, *et al.,* "Nb_3Sn coating of high purity Nb cavities", *IEEE Transactions on Magnetics,* vol. 25(2), pp. 1862–1864, 1989.